MOLECULAR AND CELLULAR BIOLOGY, Jan. 2006, p. 548–558 Vol. 26, No. 2
0270-7306/06/$08.00+0 doi:10.1128/MCB.26.2.548–558.2006

Elimination of Epiplakin by Gene Targeting Results in Acceleration of Keratinocyte Migration in Mice

Mizuki Goto,[1] Hideaki Sumiyoshi,[1] Takao Sakai,[2] Reinhard Fässler,[2] Shihoka Ohashi,[3] Eijiro Adachi,[3] Hidekatsu Yoshioka,[1] and Sakuhei Fujiwara[1]*

Department of Anatomy, Biology and Medicine (Dermatology and Biochemistry), Faculty of Medicine, Oita University, Hasama-machi, Yufu 879-5593, Japan[1]; Department of Molecular Medicine, Max Planck Institute for Biochemistry, 82152 Martinsried, Germany[2]; and Department of Molecular Morphology, Kitasato University Graduate School of Medicine, Sagamihara, Kanagawa 228-8555, Japan[3]

Received 25 February 2005/Returned for modification 15 April 2005/Accepted 8 October 2005

Epiplakin (EPPK) was originally identified as a human epidermal autoantigen. To identify the function of epiplakin, we generated epiplakin "knockout" mice. These mice developed normally, with apparently normal epidermis and hair. Electron microscopy after immunostaining revealed the presence of EPPK adjacent to keratin filaments in wild-type mice, suggesting that epiplakin might associate with keratin. The appearance and localization of keratin bundles in intact epidermal keratinocytes of EPPK$^{-/-}$ mice were similar to those in wild-type mice. Wounds on the backs of EPPK$^{-/-}$ mice closed more rapidly than those on the backs of wild-type and heterozygous mice. The outgrowth of keratinocytes from skin explants from knockout mice was enhanced compared to outgrowth from explants from wild-type mice, even in the presence of mitomycin C, suggesting that the difference in keratinocyte outgrowth might be due to a difference in the speed of migration of keratinocytes. At wound edges in wild-type mice, EPPK was expressed in proliferating keratinocytes in conjunction with keratin 6. In EPPK$^{-/-}$ mice, no similar proliferating keratinocytes were observed, but migrating keratinocytes weakly expressed keratin 6. EPPK was coexpressed with keratin 6 in some keratinocytes in explant cultures from wild mice. We propose that EPPK might be linked functionally with keratin 6.

Epiplakin (EPPK) was originally identified as an autoantigen that reacted with serum from an individual with subepidermal blistering disease (5, 6). Human EPPK is a 552-kDa protein that is expressed not only in sheets of epidermis and the esophagus, but also in the outer root sheath of hair follicles and in mucous epithelial cells (7).

Epiplakin is homologous to plectin and other members of the plakin family, but it belongs to a novel category of plakins because of the following unusual features (Fig. 1). Human epiplakin has 13 domains, and mouse epiplakin has 16 domains, that are homologous to the B domain, which is one of the plakin repeat domains (PRDs) found in the carboxy-terminal region of desmoplakin, and these domains are distributed along the amino acid sequence with relatively uniform spacing (7, 21). The amino acid sequences of the last five (human) or eight (mouse) of these B domains, starting from the carboxyl terminus, together with their associated linker regions, are particularly strongly conserved. Epiplakin lacks the coiled-coil rod domain and the amino-terminal domain that are found in all other known members of the plakin family. Furthermore, there is no dimerization motif in the entire amino acid sequence. Thus, it is likely that EPPK exists in vivo as a single-chain structure (7). The unique features of the repeated structures in EPPK undoubtedly contribute to the protein's function in vivo.

It seems likely that the carboxy-terminal regions, including PRDs and linker regions, of proteins in the plakin family, such as desmoplakin, BPAG1 (an autoantigen of bullous pemphigoid), and plectin (a protein responsible for epidermolysis bullosa with muscular dystrophy), bind to intermediate filaments (8, 12, 17, 18, 22, 23, 28). However, EPPK has only one kind of PRD, a B domain, and connecting linker domains, as noted above, and in vitro experiments have demonstrated that the EPPK plakin repeat domain with its connecting linker domain binds to intermediate filaments (10).

It is unclear why autoantibodies against epiplakin are associated with subepidermal blistering disease. Gene targeting of BPAG1 and of plectin, both of which are members of the plakin family, causes skin fragility and the formation of blisters (9, 16). We designed the present study to examine what happens when expression of EPPK is disrupted in mice.

The open reading frame that encodes EPPK is transcribed as a single exon in human and mouse (21, 25), although in the mouse, the 5′-terminal untranslated mRNA is encoded by an adjacent exon (referred to here as the first exon). Thus, no splice variants of EPPK should exist, depending on the tissue in which EPPK is expressed. Moreover, there are no genes for orthlogs with structural homology to EPPK that might compensate for the absence of EPPK, other than the gene for plectin, in the mouse and human genomes. Thus, we were able to examine whether a change in phenotype would occur when we inactivated the gene for EPPK in mice.

We report here the first gene targeting of EPPK, to our knowledge, and an analysis of some aspects of the phenotype of EPPK knockout mice. We also examined the localization of epiplakin in the murine epidermis by immunostaining and electron microscopy.

* Corresponding author. Mailing address: Department of Anatomy, Biology and Medicine (Dermatology), Oita University, Idaigaoka 1-1, Hasama-machi, Yufu 879-5593, Japan. Phone: 81-97-586-5882. Fax: 81-97-586-5889. E-mail: fujiwara@med.oita-u.ac.jp.

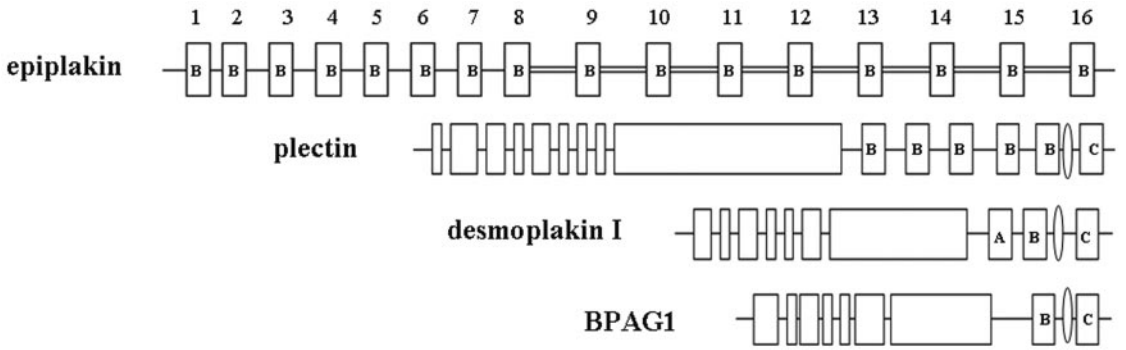

FIG. 1. Schematic representations of mouse EPPK and related members of the plakin family from human (13, 21). The double-lined linker regions and the eight B domains (domains 9, 10, 11, 12, 13, 14, 15, and 16) to their right are almost perfectly identical. Coiled-coil rod domains and amino-terminal domains are shown as open boxes. Such domains are found in plectin, desmoplakin I, and BPAG1, but they are not found in epiplakin. The domain structures of the carboxy-terminal ends of the three plakins are shown as boxes that are labeled A, B, or C. Linker subdomains between B and C domains in desmoplakin, BPAG1, and plectin are indicated with thin ovals.

MATERIALS AND METHODS

Cloning of the targeting vector. We used the mouse cDNA sequence that is homologous to the human gene for EPPK, as identified in a BLAST search (http://www.ncbi.nlm.nih.gov/BLAST/), as a probe to identify the mouse gene for EPPK in a mouse genomic library (Lambda FIX II Library; Stratagene, La Jolla, CA). Positive clones were subjected to digestion with restriction enzymes. We inserted the β-gal-Neo cassette into the second exon of the gene for EPPK to generate EPPK-null mice. Homologous recombination in mouse embryonic stem (ES) cells allowed us to replace the second exon with the modified second exon (21). We also constructed an "outside" probe that corresponded to the region between the KpnI and XbaI sites for selection of knockout ES cells (Fig. 2a).

Generation of knockout mice. The NotI-linearized targeting vector was introduced by electroporation into cultured mouse ES cells as described previously (4). Positive clones were selected with G418 and screened by Southern blotting.

Appropriate ES cells were microinjected into blastocysts obtained from C57BL/6J mice, and the blastocysts were then transferred to pseudopregnant mice. The resultant chimeric animals were mated with wild-type C57BL/6J mice to examine the germ line transmission of the targeted EPPK allele. Heterozygotes were cross-bred to produce $EPPK^{-/-}$ homozygous animals.

Genotyping of selected ES cells and mice. We examined the genotypes of clones of ES cells and of animals by Southern blotting. We extracted DNA from cells and mouse tissue as follows. We incubated ES cells or mouse tissue in cell lysis buffer (100 mM Tris-HCl, pH 7.5, 5 mM EDTA, 0.2% SDS, 200 mM NaCl) with 0.4 mg/ml proteinase K at 55°C for 3 h. After extraction with phenol and chloroform, DNA was precipitated in ethanol. Southern blotting was performed with samples of genomic DNA that had been digested with the restriction endonuclease HindIII and, as a probe, a [^{32}P]dCTP-labeled 0.2-kbp fragment of DNA obtained from a genomic subclone that had been digested with KpnI and XbaI (Fig. 2a). The probe recognized a 19-kbp fragment of wild-type mouse DNA and a 15-kbp fragment of DNA from ES cells that had undergone homologous recombination with the targeting vector (Fig. 2b).

Reverse transcription-PCR (RT-PCR). For RT-PCR, we extracted total RNA from the skin of wild-type mice and $EPPK^{-/-}$ mice using ISOGEN (Nippon Gene, Tokyo, Japan). We used the following primers, which were specific for the mouse gene for EPPK: 5′-TAC CAC ACA CGA TCG TCT TG-3′ (pr93) and 5′-CTC CTC CGG TCC TCT GTG AA-3′ (pr95). As primers for the control amplification by RT-PCR of mRNA for β-actin, we used the primers 5′-AAG AGA GGT ATC CTG ACC CT-3′ (forward) and 5′-TAC ATG GCT GGG GTG TTG AA-3′ (reverse). The conditions for RT-PCR were as follows: 1 cycle at 94°C for 90 s; 35 cycles of 60 s at 94°C, 60 s at 55°C, and 180 s at 72°C; and a final extension at 72°C for 450 s.

Expression of a fusion protein and preparation of polyclonal antibodies. The glutathione *S*-transferase–EPPK fusion protein, which encodes the linker region between the 15th and 16th B domains (Fig. 1), and polyclonal antibodies were made as in the previous study (7).

Wound repair and explant culture. Mice were anesthetized with an intraperitoneal injection of ketamine and xylazine. The dorsal surface was shaved, and a disposable 0.6-cm-diameter skin punch biopsy tool (Health Link, Jacksonville, FL) was used to create a full-thickness excision wound that extended to the fascia. The diameter of the wound was measured daily after removal of the scab over the wound.

For explant cultures, 2- or 4-day-old pups were decapitated. The bodies were washed with 70% ethanol in a tissue culture hood. The limbs were removed, and a full-thickness incision was made in the anterior-to-posterior direction on the ventral surface. The skin was peeled away with forceps, and for the preparation of explants without dermis, the skin was floated on a 0.25% solution of trypsin in phosphate-buffered saline (PBS) that included 0.5 mM EDTA for 5 h at 4°C. After the dermis had been removed, the epidermis was washed in medium, cut with a sterile 4-mm punch biopsy tool, and then cultured as full-thickness explants according to the method described by Mazzalupo et al. (15). The explants were placed individually in the wells of a 24-well untreated tissue culture dish. After waiting 60 min for the skin to adhere to the base of each well, we added 200 μl of medium per well and incubated the dish at 37°C in an atmosphere of 5% CO_2 in air (day 0). On day 1, the explants were submerged by adding 1.5 ml of medium to each well. The medium was replaced at 2- to 3-day intervals thereafter (15). A subset of explants was treated with mitomycin C (10 μg/ml for 2 h; Sigma-Aldrich, St. Louis, MO) 24 h after being seeded, and their diameters were measured after 7 days in the presence of the drug (30). We used the NIH Image System to measure mean distances from the edge of each explant to the leading edge and the area of outgrowth.

Histology. For histopathological studies, samples of skins of mice were fixed in 4% paraformaldehyde, washed in PBS (pH 7.4), and then passed through an ethanol series (50%, 75%, 85%, 95%, and 100%). Then, 4-μm sections were stained with hematoxylin and eosin and examined under a light microscope.

Immunohistochemical staining of normal skin, of wounded skin, and of explants. For immunohistochemical staining of EPPK, skin was fixed as described above and sections (3 μm) were incubated with polyclonal antibodies against mouse EPPK at a dilution of 1:2,560 and then with horseradish peroxidase-conjugated antibodies (LSAB 2 System HRP; DAKO, Carpinteria, CA). Then, the tissues were treated with diaminobenzidine as a chromogen and examined by light microscopy. Wounded skin and explants were fixed in 3% paraformaldehyde for 10 min and then passed through a graded methanol series (50%, 75%, and 100%). After removal of the methanol by incubation in a second graded methanol series (75%, 50%, and 25%), washing with PBS, and incubation with blocking solution (10% goat serum, 20 mg/ml bovine serum albumin, 1% Triton X-100, and 1% dimethyl sulfoxide in PBS), samples were incubated with mouse monoclonal antibody against keratin 6 (Abcam Ltd., Cambridge, United Kingdom) and rabbit antibodies against mouse EPPK for 1 h. Then, the samples were incubated with fluorescein isothiocyanate-conjugated goat antibodies against mouse immunoglobulin G (IgG) (Molecular Probes, Eugene, OR) and rhodamine-conjugated goat antibodies against rabbit IgG (Molecular Probes) for 30 min. Samples were examined using a laser scanning confocal microscope (LSM5 PASCAL; Carl Zeiss, Germany). To identify the nuclei of keratinocytes, samples were treated with 4′,6-diamidino-2-phenylindole dihydrochloride (DAPI) (Dojindo, Kumamoto, Japan). To assess the distribution of involucrin in the epidermis, goat polyclonal antibody against involucrin of mouse origin (Santa Cruz Biotechnology, Inc., Santa Cruz, CA) was used.

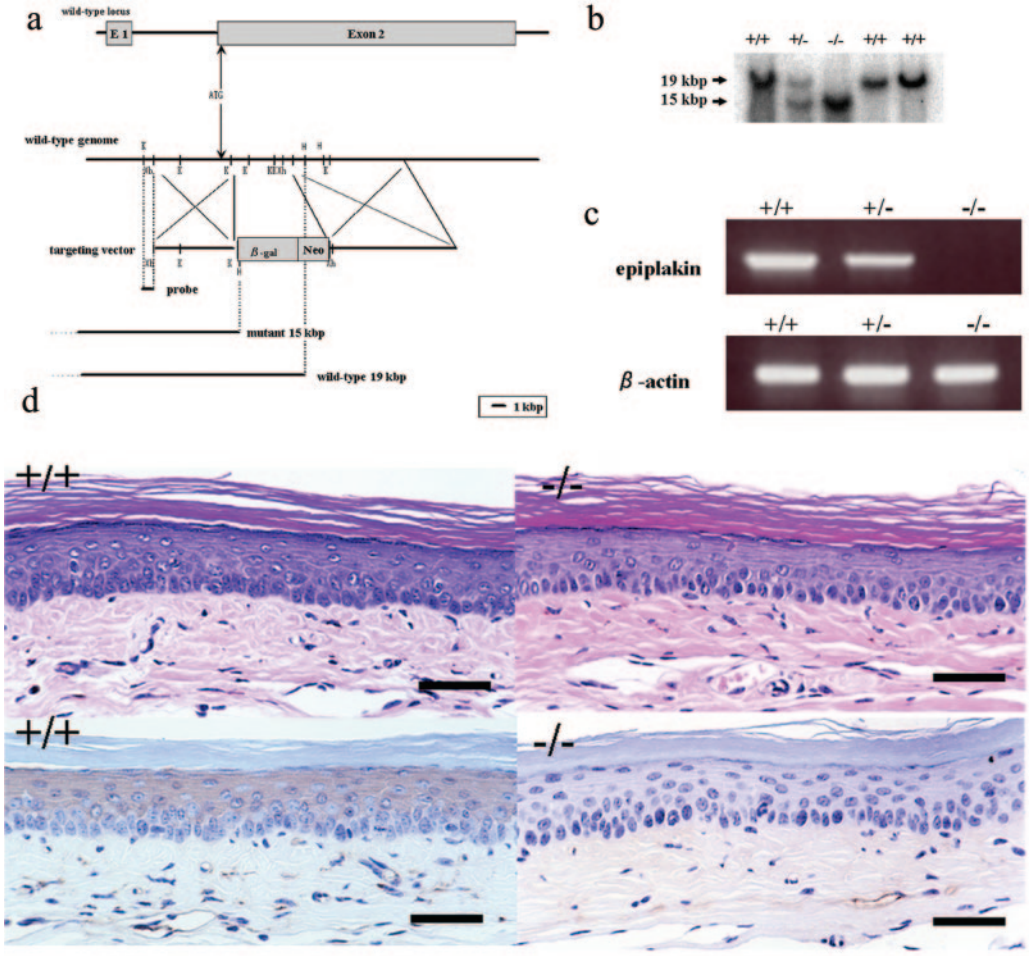

FIG. 2. (a) The β-gal-Neo cassette was inserted into the second exon of the mouse gene for EPPK to generate the targeting vector used for generation of EPPK$^{-/-}$ mice. As a result of homologous recombination in mouse ES cells, this construct replaced the second exon of the wild-type gene. The "outside" probe was generated by cleavage at the KpnI and XbaI sites for selection of ES cells and mice by genomic Southern blotting. K, KpnI; H, HindIII; Xb, XbaI; Xh, XhoI. (b) Southern blotting yielded a 19-kbp DNA fragment in the case of the wild-type allele and a 15-kbp fragment in the case of the mutant allele. Heterozygous animals harbored both alleles. (c) Wild-type and heterozygous skin cells expressed EPPK mRNA, whereas EPPK$^{-/-}$ cells did not express this mRNA. All cells expressed β-actin mRNA.(d) Histology of skin of the feet. Staining with hematoxylin and eosin revealed the absence of blistering in both wild-type and EPPK$^{-/-}$ mice (top). Immunostaining with polyclonal antibodies against the linker region of EPPK was negative in EPPK$^{-/-}$ skin, while it was positive in wild-type skin (bottom). Bars = 50 μm.

Electron microscopy. Small blocks of mouse skin were placed in Zamboni's fixative at 4°C for 2 h and then treated as described previously by Yamamoto-Hino et al. (31). In brief, cryosections on glass slides were incubated overnight with antibodies against mouse EPPK or mouse monoclonal antibody against keratin 6, which had been diluted 100-fold. Then they were treated with antibodies raised in goat against rabbit or mouse IgG, which had been conjugated with 0.8-nm particles of colloidal gold (Aurion Co., Ltd., Amsterdam, The Netherlands). The sections were soaked in a mixture of 2.5% glutaraldehyde, 0.2% tannic acid, and 1% OsO_4 in 0.1 M phosphate buffer for 30 min at room temperature and then rinsed in triple-distilled water. They were then incubated with a solution for silver enhancement (Aurion Co., Ltd.), embedded in a 1% solution of chitosan, fixed in 2.5% glutaraldehyde, and subjected to routine processing. Finally, the thin sections were stained with uranyl acetate and lead citrate and examined with an electron microscope (JEM 1230; JEOL Ltd., Tokyo, Japan).

RESULTS

Generation of mice with an inactivated gene for EPPK. Our strategy for disruption of the expression of the gene for EPPK involved construction of a gene-targeting vector that would allow us to generate EPPK-null mice. We anticipated that the mutation would result in a premature termination codon in exon 2 at a distance of approximately 0.5 kbp from the ATG codon. Thus, almost every function of mouse EPPK would be disrupted (Fig. 2a). After electroporation of ES cells with the targeting vector, we selected positive clones by growing cells in medium that contained the neomycin analog G418. We confirmed that homologous recombination had occurred between the wild-type allele and the targeting vector by Southern blotting using DNA digested with KpnI and XbaI. A 15-kbp fragment indicated the presence of the disrupted allele, whereas a 19-kbp fragment corresponded to the wild-type allele (Fig. 2b).

We microinjected ES cells with the appropriately disrupted gene into C57BL/6J blastocysts. The resultant chimeric males provided evidence of germ line transmission of the ES cell genome, as revealed by the agouti coat color of offspring from chimeras. An inbred line was established by mating the chimeras with 129/Sv mice. Heterozygous animals were also generated with a pure 129/Sv background.

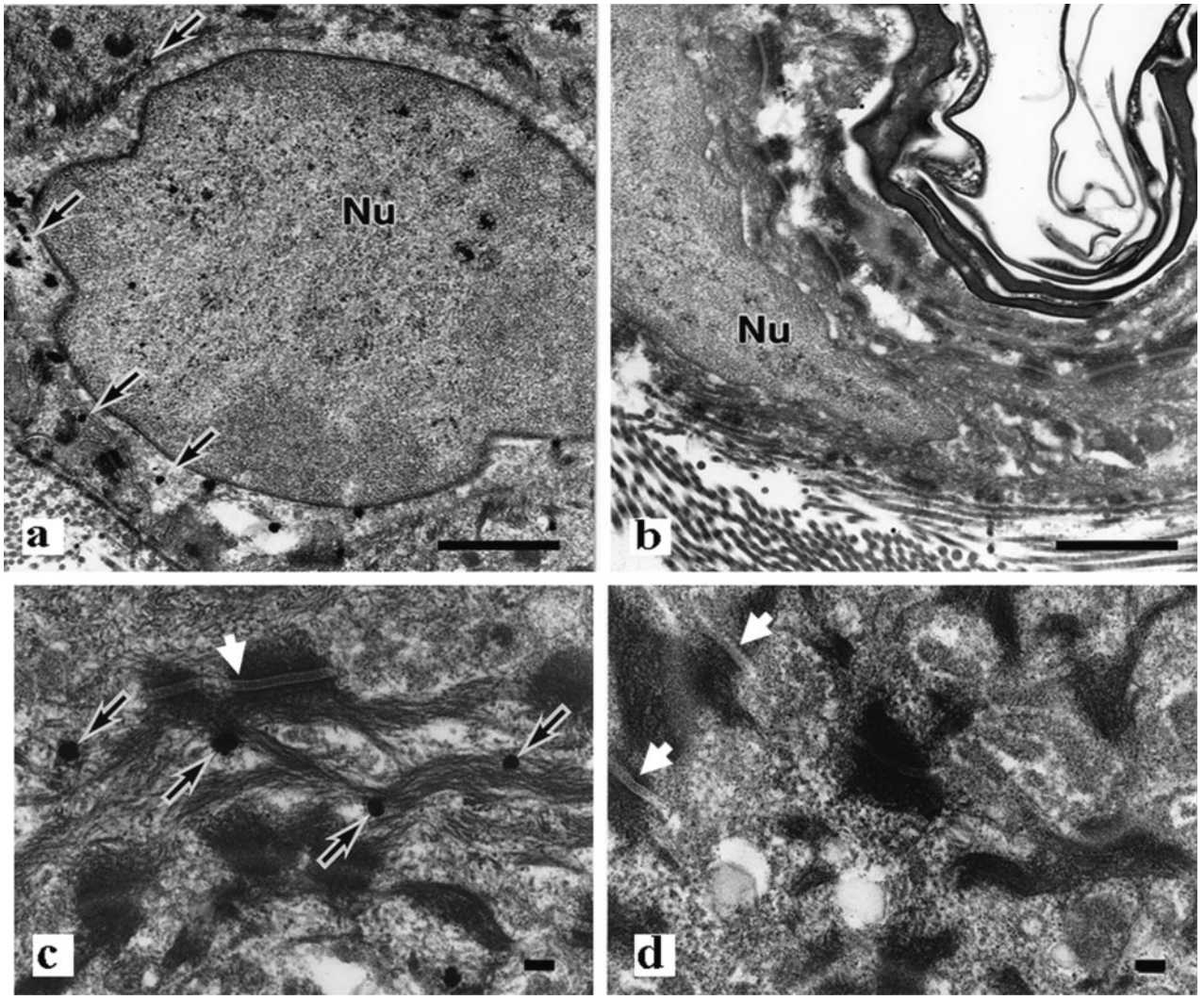

FIG. 3. Electron micrographs of keratinocytes from the dorsal epidermis with low (a and b) and high (c and d) magnification. There are no apparent abnormalities in the keratin filaments and desmosomes (white arrows) of wild-type mice (a and c) and EPPK$^{-/-}$ mice (b and d). Silver grains are visible adjacent to keratin bundles (black arrows). Nu, nucleus. Bars = 1 μm (a and b) and 100 nm (c and d).

We confirmed that the mice lacked a gene for full-length EPPK by genomic Southern blotting, RT-PCR, and immunostaining with polyclonal antibodies (Fig. 2b, c, and d).

EPPK$^{-/-}$ mice resembled wild-type mice. The EPPK$^{-/-}$ mice resembled wild-type mice in terms of gross phenotype, and light microscopy revealed the absence of blistering and skin fragility (Fig. 2d). Mice that were homozygous for the targeted allele were born at the expected Mendelian frequency. They developed normally and were healthy and fertile. In mice, EPPK has been found by immunostaining, not only in skin, but also in hair follicles, the esophagus, and the simple epithelium of the digestive organs, as is also the case in humans (7, 21). However, there were no abnormalities in such tissues of EPPK$^{-/-}$ mice at the macroscopic and light-microscopic levels (data not shown). Under the electron microscope, there were no apparent differences between basal and spinous keratinocytes, respectively, of EPPK$^{-/-}$ mice and wild-type mice (Fig. 3a, b, c, and d). Immunoreactivity specific for EPPK was detected adjacent to keratin filaments in wild-type mice, suggesting that epiplakin might be associated with keratin. However, the appearance and localization of keratin bundles in intact epidermal keratinocytes of EPPK$^{-/-}$ mice were similar to those in wild-type mice. Immunoreactivity in wild-type mice was detected from the basal cells to the granular cells and was not concentrated in desmosomes or hemidesmosomes (data not shown).

EPPK$^{-/-}$ mice exhibited slightly enhanced wound closure. In EPPK$^{-/-}$ mice, wound closure was almost complete on day 10, whereas in wild-type and heterozygous mice, wound closure occurred 1 or 2 days later (Fig. 4). We postulated that the migration and/or proliferation of mouse keratinocytes might have been accelerated in the absence of EPPK. We confirmed our observations under the light microscope. Enhanced wound closure was evident in EPPK$^{-/-}$ mice even when we compared wounds without peeling off the scabs. In EPPK$^{-/-}$ mice, elevated numbers of keratinocytes were observed, and they migrated under the fibrin clot on day 3. By contrast, in wild-type mice, fewer keratinocytes were localized on the upper side of

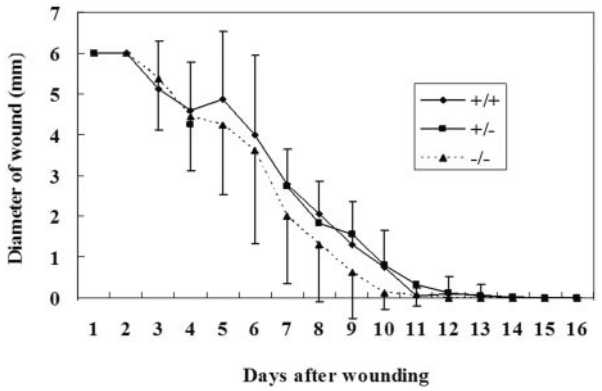

FIG. 4. Comparison of wound closure processes between wild-type, heterozygous, and homozygous mice. In EPPK$^{-/-}$ mice, wound closure occurred slightly faster than in wild-type and heterozygous mice (n = 28 for wild-type, 56 for heterozygous, and 20 for EPPK$^{-/-}$ mice). The error bars represent standard deviations.

the wound's edge on day 3. On day 4, the difference between the two lines of mice was quite marked (Fig. 5). In wild-type mice, the edges of wounds invaginated sharply, the epidermis was hypertrophic, a few keratinocytes made a wall, and small populations of keratinocytes migrated under the clot. A large scab covered the ulcer. By contrast, in EPPK$^{-/-}$ mice, we observed decreased hypertrophy of the epidermis at the wound's edge, and the leading edge extended a long distance compared with that in wild-type mice. The scab peeled away from the edge of the wound, becoming smaller and shifting to the center of the wound.

During wound healing, synthesis of keratin 6 is induced in suprabasal keratinocytes. In the wound edge, keratin 6 was strongly expressed in wild-type mice, while in EPPK$^{-/-}$ mice, keratin 6 expression was much weaker (Fig. 6b and c). Next, we examined the expression of EPPK and compared it to that of keratin 6 in wild-type mice by immunohistochemical staining. Around the region of the wound, EPPK was expressed in the upper half of the epidermis, but expression of EPPK was suppressed in the granular layer of the epidermis, as is the case in normal epithelium (Fig. 6d). On the basilar side of the suprabasal layer of the epidermis at the wound's edge, where keratin 6 was expressed and EPPK was expressed only weakly, keratinocytes were small (Fig. 6e and f). In the upper layer of the epidermis, EPPK was expressed strongly, especially in larger keratinocytes, but unevenly (Fig. 6f, g, and h). In the granular layer at the edge of the wound in wild-type mice, neither epiplakin nor keratin 6 was expressed (Fig. 6k). By contrast, in EPPK$^{-/-}$ mice, the epithelium was only slightly hypertrophic (Fig. 6i) and keratin 6 was weakly expressed in the upper layer of the wounded area (Fig. 6j). In the upper and lower regions, the keratinocytes exhibited none of the morphological changes seen in wild-type mice. At the leading edge, only keratin 6 was expressed, even in wild-type mice, and there were no morphological differences between wild-type and knockout mice. Involucrin was distributed in the suprabasal layer in the epidermis, including the granular layer, while EPPK was expressed only in the upper half-layer of the epidermis, with the exception of the granular layer (Fig. 6l and m).

After immunostaining, electron microscopy revealed that at wound edges in EPPK$^{-/-}$ mice, antibodies against keratin 6 reacted far less strongly than in wild-type mice. This observation suggested that, in EPPK$^{-/-}$ mice, the expression of keratin 6 was suppressed at the wound edge (Fig. 7).

On the appearance of the final scar, the epidermis in wild-type mice was more hypertrophic than that in EPPK$^{-/-}$ mice (data not shown).

EPPK$^{-/-}$ keratinocytes had an enhanced capacity for epithelialization. Epiplakin is expressed only in the epithelium in normal skin. Thus, it is likely that EPPK contributes to the epithelial closure of wounds. To assess the wound epithelialization potential in EPPK$^{-/-}$ mice, we used a skin explant assay in which cultured explants mimic the behavior of keratinocytes at the edges of skin wounds in vivo. This assay allows the qualitative and quantitative assessment of the potential of keratinocytes for epithelialization while avoiding the effects of dermis-mediated contraction of the wound bed (3, 15). We found that EPPK$^{-/-}$ explants exhibited a statistically significant 1.2-fold enhancement of epithelial outgrowth compared with explants from wild-type and heterozygous mice (Fig. 8a and b).

Enhanced outgrowth of the EPPK$^{-/-}$ keratinocytes resulted from migration. Reepithelialization of skin wounds in vivo results from increases in mitotic activity and the migration of keratinocytes that are located at wound margins (14). Similarly, over a period of 7 days in culture, migration and mitosis contribute equally to the outgrowth of keratinocytes from skin explants (27). To determine whether migration or mitosis was involved in the effect of EPPK, we assessed the outgrowth of keratinocytes after treatment of explants with mitomycin C, an irreversible inhibitor of mitosis (27). Relative to the wild-type and heterozygous controls, treated and untreated EPPK$^{-/-}$ explants exhibited similar outgrowth of keratinocytes in terms of both distance and area (Fig. 8c and d). However, treated EPPK$^{-/-}$ skin explants exhibited a statistically significant 1.5-fold enhancement of epithelial outgrowth compared to wild-type and heterozygous explants. Untreated EPPK$^{-/-}$ skin explants exhibited a statistically significant 1.2-fold enhancement of epithelial outgrowth compared with wild-type and heterozygous explants.

Epiplakin was coaligned with keratin 6 in some keratinocytes in wild-type explants. In order to investigate the colocalization of epiplakin and keratin 6, we examined explant cultures with a confocal microscope after double immunostaining with antibodies against keratin 6 and EPPK. In wild-type explants, epiplakin was distributed as granules or a reticular network in almost all keratinocytes, and keratin 6 was distributed as a fine reticular network and only partially as filaments in some keratinocytes. In some keratinocytes, EPPK was colocalized with keratin 6 (Fig. 9a to f). Since actin filaments are thought to be involved in cell migration, we observed explants from wild-type mice after double immunostaining with antibodies against EPPK and actin. Epiplakin was not colocalized with actin (data not shown). In EPPK$^{-/-}$ explants, keratin 6 was distributed as filaments that seemed to be stretched in a large number of keratinocytes (Fig. 9g and h).

DISCUSSION

Epiplakin is a member of the plakin family, to which plectin and BPAG1 also belong. Mice that lack plectin or BPAG1

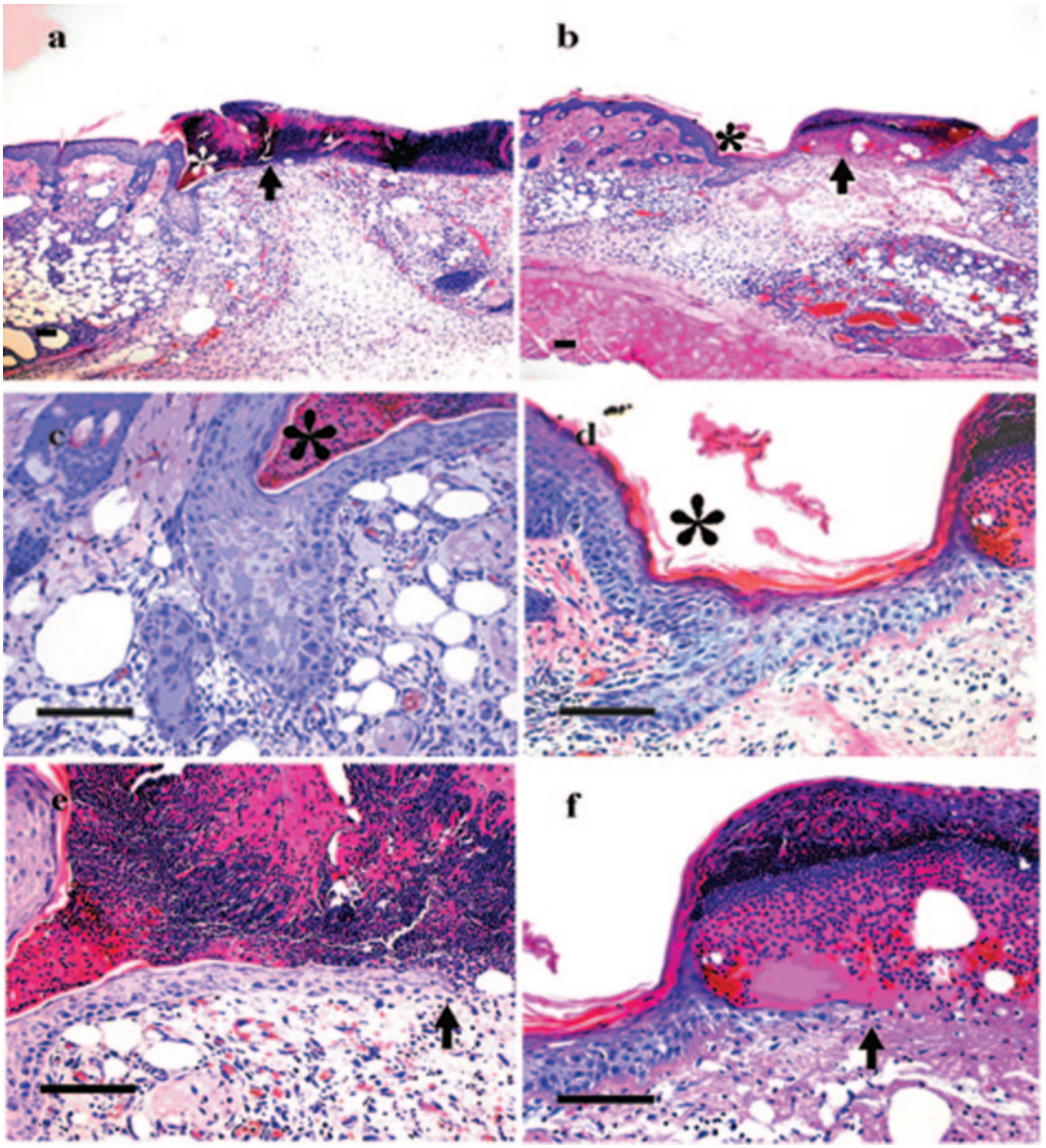

FIG. 5. Histological analysis of skin wounds on the backs of wild-type (a, c, and e) and EPPK$^{-/-}$ (b, d, and f) mice. On day 4, the edges of wounds in wild-type mice invaginated sharply, and the epidermis was hypertrophic at the margins (a). A large scab covered the ulcer. In EPPK$^{-/-}$ mice, there was decreased hypertrophy of the epidermis at the wound's edge, and the leading edge extended a long distance compared with that in wild-type mice. The scab was also smaller than that in wild-type mice (b). *, wound edge; arrows, leading edge. Higher-magnification views of the wound edge (c and d) and of the leading edge (e and f) are shown. Bars = 100 μm.

have fragile skin (1, 9). However, EPPK$^{-/-}$ mice exhibited no skin fragility up to 2 years of age, and light microscopy revealed no signs of blistering of the skin. Moreover, under the electron microscope, we found no abnormalities in the epidermal keratinocytes. The absence of EPPK might have an effect on skin fragility different from that of the absence of BPAG1 and plectin because the latter proteins are localized in hemidesmosomes in basal cells and connect intermediate filaments and hemidesmosomes (9, 16). Ultrastructural analysis suggested that EPPK is not concentrated in desmosomes and hemidesmosomes but is associated with keratin filaments in the cytoplasm of epidermal keratinocytes. Jang et al. reported recently that in cultured HeLa cells, HaCaT cells, and human keratinocytes, EPPK is colocalized with keratin and vimentin, and in dot blot experiments, the plakin repeat domain with its linker bound to the intermediate filaments (10). These data support the validity of our findings.

Epiplakin and plectin have a common domain structure at their carboxyl termini, but plectin did not appear to compensate for the loss of EPPK, since in EPPK$^{-/-}$ mice, the pattern of immunostaining for plectin was similar to that in wild-type mice (data not shown).

Epiplakin is expressed not only in the skin, but also in hair follicles, the esophagus, and the simple epithelium of digestive organs (7, 21). Jang et al. suggested, from knock-down experiments, that the effect of elimination of EPPK might be more

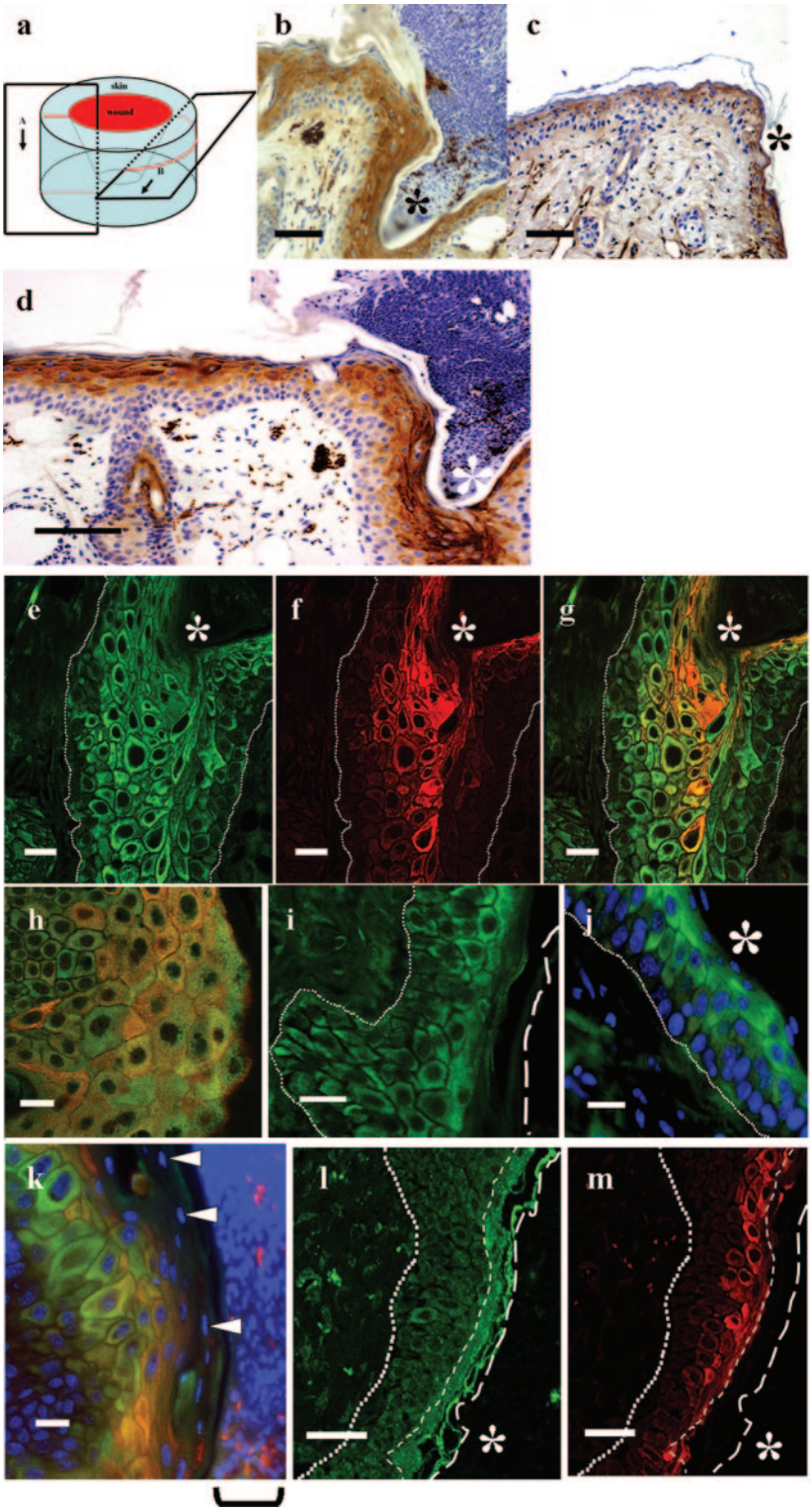

FIG. 6. Immunohistochemical study of the skin wounds of wild-type (b, d, e to h, and k to m) and EPPK$^{-/-}$ (c, i, and j) mice. Vertical views of the hypertrophic epidermis around the wound edge (b to d) and at the wound edge (e to g and j to m), as indicated by plane A in scheme a, and horizontal views of wound edges (h and i), as indicated by plane B in scheme a, are shown. Light-microscopic (b to d), confocal-microscopic (e to i, l, and m), and immunofluorescence-microscopic (j and k) images are shown. Around the wound edge, in the hypertrophic epithelium of wild-type mice, keratin 6 was expressed in the suprabasal layer (b). By contrast, around the wound edge of EPPK$^{-/-}$ mice, keratin 6 was weakly expressed in the upper half of the epidermis (c). EPPK was strongly expressed in the upper half, with the exception of the granular layer in wild-type mice (d). After immunostaining of the wound edge with keratin 6 (green), almost the entire suprabasal layer was stained (e). In the wounded area, EPPK (red) was strongly expressed throughout the middle region, with the exception of the granular layer (f). Merged images (g and h) showed only larger epidermal cells that coexpressed both keratin 6 and epiplakin. At higher magnification of the wound edge, immunostaining of EPPK

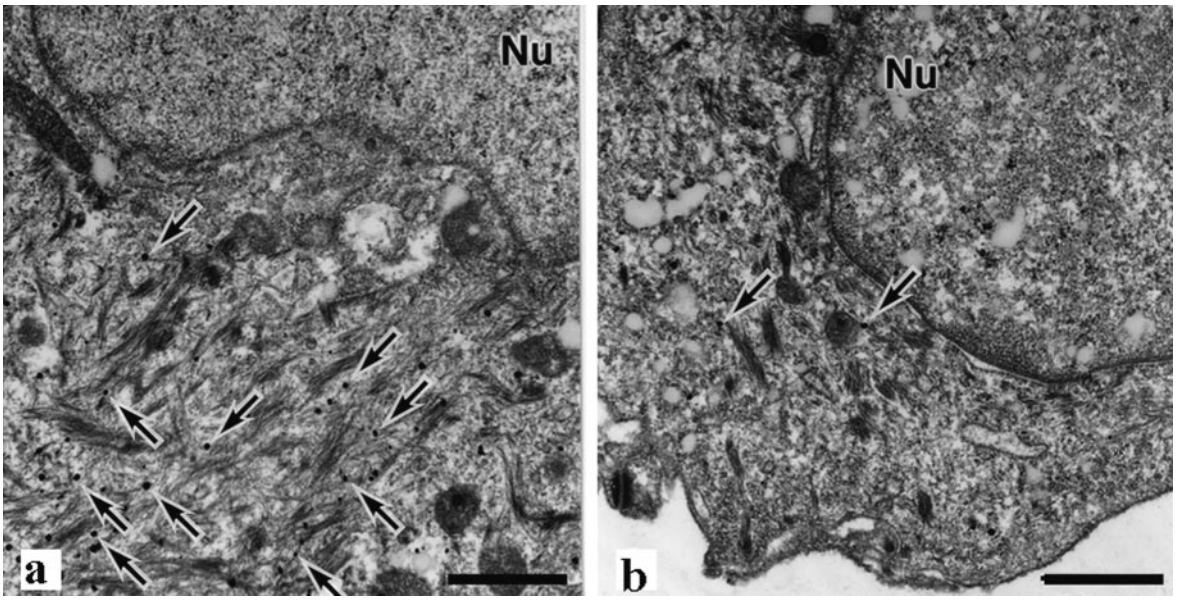

FIG. 7. Electron micrographs of suprabasilar keratinocytes at wound edges. Immunostaining for keratin 6 (silver grains indicated by arrows) was much weaker in EPPK$^{-/-}$ mice (b) than in wild-type mice (a). Nu, nucleus. Bars = 1 μm.

apparent in the simple epithelium than in keratinocytes or HaCaT cells (10). However, in EPPK$^{-/-}$ mice, we found no abnormalities in such tissues by light microscopy (data not shown). Moreover, although it has been reported that EPPK is cross-linked with trichohyalin in mouse hair follicles (24), the hairs of EPPK$^{-/-}$ mice seemed normal. In our study, the immunoreactivity of EPPK was not detected in the granular layer of the epidermis. Jang et al. suggested that in the later stages of keratinocyte differentiation, epiplakin continues to be synthesized with some degradation (10). This discrepancy might have occurred because the EPPK epitope was masked due to transglutaminase-mediated cross-linking, while the involucrin epitope was not disturbed in the granular layer.

The enhanced wound healing in EPPK$^{-/-}$ mice was unexpected. When the skin is undamaged, EPPK appears to be unnecessary, and other molecules can perform its role in its absence. However, when the integrity of normal skin is disrupted, proliferating keratinocytes express enhanced amounts of EPPK. At the wound edge in wild-type mice, expression of keratin 6 was induced first in relatively small keratinocytes in the suprabasal portion of the epidermis. Later, expression of EPPK was induced in larger keratinocytes. The edge of the wound was fixed by these cells as if by a wall. In EPPK$^{-/-}$ mice, we found no such large keratinocytes and no wall at the wound's edge, and the keratinocytes appeared to have migrated more rapidly under the scab. As the leading edges progressed, the scab peeled off from the wound's edge and regressed. At the front of the leading edge, only keratin 6 and no epiplakin was expressed, and the cells were similar in wild-type and EPPK$^{-/-}$ mice. The data from skin explant cultures supported the observed difference in wound healing between wild-type and EPPK$^{-/-}$ mice. In the presence of mitomycin C, which inhibits mitosis, EPPK$^{-/-}$ explants also exhibited enhanced outgrowth compared to wild-type and heterozygous explants. It seems likely that the contribution of EPPK$^{-/-}$ keratinocytes to the enhanced outgrowth of explants was due to the migration of keratinocytes rather than to their proliferation. Some proliferating and migrating cells came from the outer root sheaths of hair follicles, but the patterns of immunostaining of keratin 6 and EPPK were essentially similar to those in cells of epidermal origin.

The mechanism responsible for the faster migration of keratinocytes is unknown. Epiplakin was expressed in proliferating large keratinocytes, namely, differentiated keratinocytes at the wound's edge, in wild-type mice, but at the wound's edge in EPPK$^{-/-}$ mice no such large keratinocytes were observed. The migratory process is presumably mediated by actin filaments and microtubules (11). However, EPPK was apparently not coaligned with actin or with microtubules (unpublished data). Spectraplakin binds to actin and microtubules and perhaps to intermediate filaments (11, 20), while EPPK has neither an actin-binding site nor a microtubule-binding domain. How-

was more evident in larger keratinocytes, but staining was uneven (h; right, scab side) At wound edges in EPPK$^{-/-}$ mice, the epidermis was only slightly hypertrophied, and keratin 6 was weakly expressed in the upper region of the epidermis (i and j; stained for keratin 6 and with DAPI). After staining with DAPI (blue), in addition to double immunostaining, neither keratin 6 nor epiplakin was detected in the granular layer, as indicated by arrowheads (k; the square bracket indicates the scab). Involucrin (green in panel l) was distributed in the suprabasal layer of the epidermis, including the granular layer, while epiplakin (red in panel m) was expressed in the upper half-layer of the epidermis, with the exception of the granular layer. *, wound edge; arrowheads, nuclei in the granular layer. The dotted lines represent basal lamina, long-dashed lines represent the surface of the stratum corneum, and short-dashed lines represent the borders of the malpighian and granular layers of the epidermis. Bars = 50 μm (b, c, l, and m), 100 μm (d), and 20 μm (e to k).

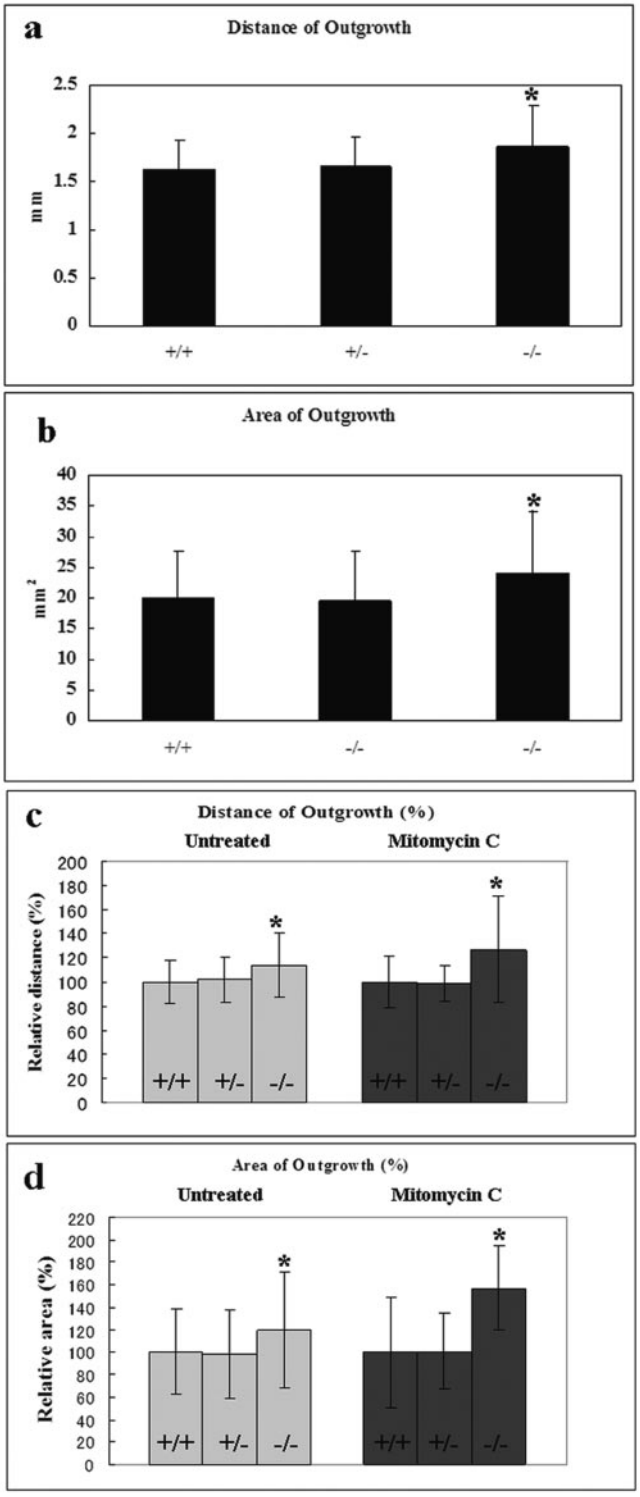

FIG. 8. Comparison of wild-type, heterozygous, and EPPK$^{-/-}$ skin explants in terms of the distance between keratinocytes located at the distal edge of the outgrowth and the edge of each explant. The error bars represent standard deviations. Asterisks indicate a statistically significant difference from the wild type ($P < 0.01$ or $P < 0.05$, as indicated below; Student's t test). (a) Comparison of the extents of outgrowth ($P < 0.01$; $n = 148$ for wild-type, 143 for heterozygous, and 144 for EPPK$^{-/-}$ explants). (b) Comparison of areas of outgrowth ($P < 0.01$; $n = 71$ for wild-type, 63 for heterozygous, and 68 for EPPK$^{-/-}$ explants). The extents and total areas of keratinocyte outgrowths after 7 days, after incubation with or without mitomycin C from 24 h onward, are shown for heterozygous, EPPK$^{-/-}$, and wild-type explants. (c) Comparison of the extents of outgrowth ($P < 0.05$; for treatment of explants with mitomycin C, $n = 15$ for wild-type, heterozygous, and EPPK$^{-/-}$ explants). (d) Comparison of areas of outgrowth ($P < 0.05$; for treatment of explants with mitomycin C, $n = 7$ for wild-type, 10 for heterozygous, and 8 for EPPK$^{-/-}$ explants).

ever, EPPK might interact with and coordinate the activities of other molecules, including members of the spectraplakin family.

Wound healing is a complex process. With respect to the expression of keratin after epidermal injury, it is known that keratins 6, 16, and 17 are expressed in suprabasal keratinocytes at the wound's edge and that such expression is suppressed once the epidermis has covered the wound (2, 3, 19). Enhanced healing of wounds was observed in keratin 6 (K6α/β) knockout mice, but such mice died soon after birth as a result of the fragility of the stress-bearing epithelium within the oral mucosa (29, 30). The common phenotype, namely, faster closure of wounds in EPPK$^{-/-}$ and K6α/β$^{-/-}$ mice, and the induced expression of both proteins at the edges of wounds suggest that EPPK might be linked functionally with keratin 6. In some cells in our explant cultures, EPPK and keratin 6 were colocalized, and in EPPK$^{-/-}$ mice, the expression of keratin 6 seemed to be suppressed in the wounded area. Epiplakin might enhance the functions of keratin 6 during wound healing, and the proteins might collaborate and contribute to the reinforcement required for resistance to increased mechanical stress. The localization patterns of K6 in the wild type and EPPK$^{-/-}$ explants were different. These data also suggest that EPPK might therefore work in collaboration with K6, although we have no direct evidence that EPPK in fact interacts with K6.

The putative type I partners of keratins 6, 16, and 17 (19) might function with EPPK. In this context, the delayed healing of wounds that is induced by elevated levels of keratin 16 is intriguing (26, 27).

We tried to detect the differences in expression pattern of other types of keratin, e.g., K5, -14, and -10, between wild-type and EPPK$^{-/-}$ mice. The staining patterns of K5, -14, and -10 in EPPK$^{-/-}$ mice were similar to those of wild-type mice, and the expression of K10 was lowered at the wound edges.

Despite several reports of the effects on wound healing of a deficiency in or overexpression of keratin in mice, as described above, there are no reports, to our knowledge, of the genetic modification of the expression of any members of the plakin family of proteins and its effect on wound healing. Our EPPK$^{-/-}$ mice should help us to clarify the involvement of intermediate filaments in the migration of keratinocytes.

In summary, we generated EPPK knockout mice by inactivating the single mouse gene for EPPK. EPPK$^{-/-}$ mice had no apparent phenotypic abnormalities, but the closure of wounds on their backs was slightly accelerated compared with that in wild-type and heterozygous mice. In the skin explant assay, EPPK$^{-/-}$ explants also exhibited accelerated migration of keratinocytes compared with that in explants of wild-type and heterozygous skin. This phenomenon might involve changes in interactions between EPPK and intermediate filaments, such as keratin. This is the first report, to our knowledge, of the

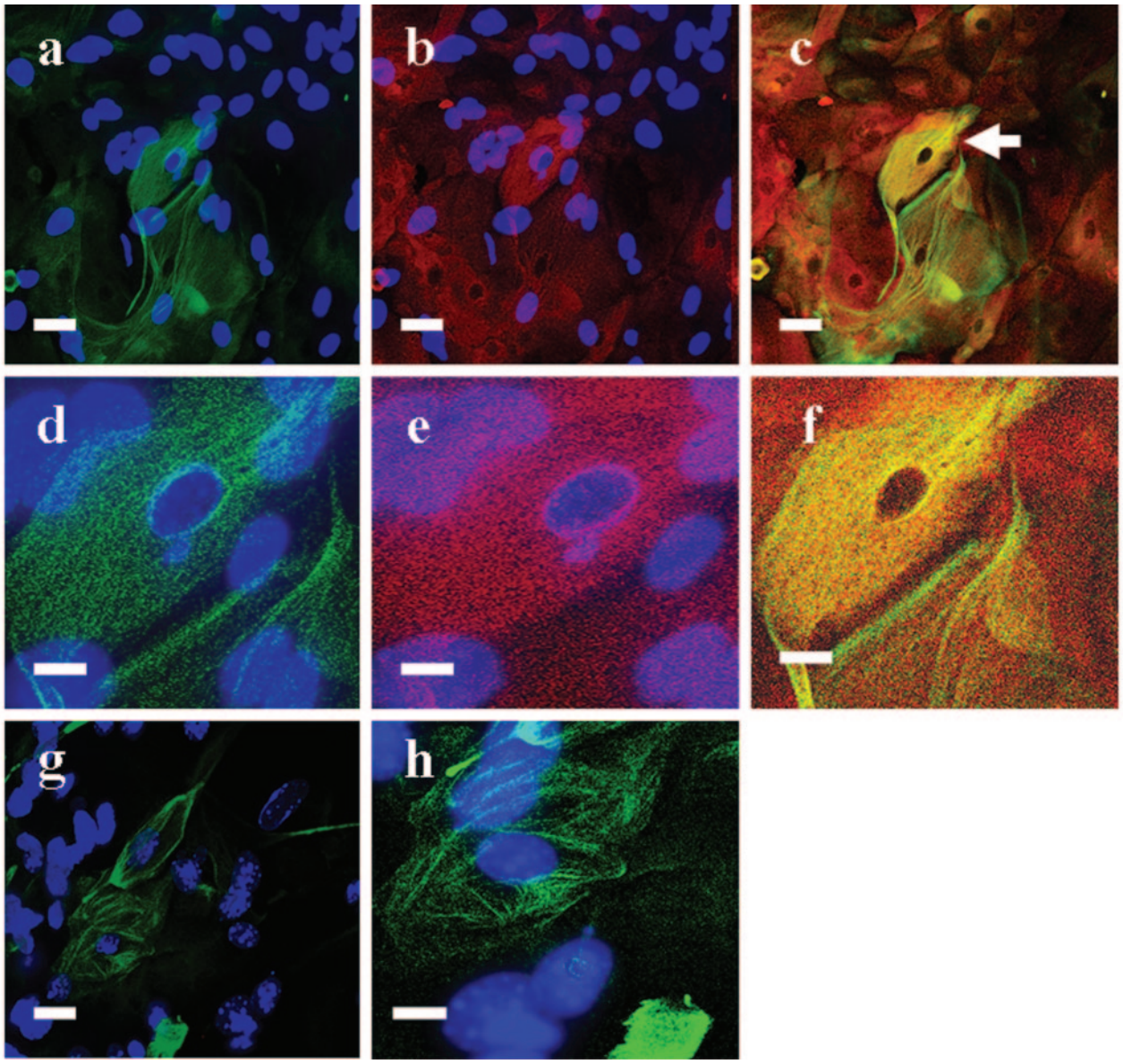

FIG. 9. Immunolocalization of keratin 6 in keratinocytes of explants from wild-type (a to f) and EPPK$^{-/-}$ (g and h) mice. In wild-type explants, keratin 6 (green) was distributed as fine reticular networks and only partly as fine filaments in some keratinocytes (a), and epiplakin (red) was distributed as granules or reticular networks in almost all keratinocytes (b). In the merged image (c), epiplakin was colocalized with keratin 6 and appeared yellow. At higher magnification, in the keratinocyte indicated by an arrow in panel c, keratin 6 (d) and epiplakin (e) were colocalized, and fine filaments or reticular networks were yellow in the merged image (f). In EPPK$^{-/-}$ explants, a large number of keratinocytes contained weakly stained filamentous and apparently stretched keratin 6 (g). At higher magnification, in the keratinocytes from EPPK$^{-/-}$ explants, the keratin 6 was distributed in a more filamentous and less reticular pattern (h). Nuclei in all panels except panels c and f were counterstained with DAPI. Bars = 50 μm (a to c and g) and 20 μm (d to f and h).

generation of EPPK knockout mice, and these mice should help us to analyze the functions of other members of the plakin family, since EPPK is an extreme example of the family, being composed almost exclusively of plakin repeat domains.

ACKNOWLEDGMENTS

We are most grateful to the late Rupert Timpl of the Max-Planck Institute for Biochemistry (Germany; Project QLK3-CT2000-00084 of Timpl) for encouraging our research; to Katsushi Owaribe (Nagoya University) for the kind gift of plectin-specific antibodies; and to Satoko Sato, Aiko Yasuda, and Hiroaki Kawasato for technical assistance.

This work was supported in part by grants 1370892 and 15591184 to S.F. from the Ministry of Education, Culture, Science and Technology of Japan.

REFERENCES

1. **Andrä, K., H. Lassmann, R. Bittner, S. Shorny, R. Fässler, F. Propst, and G. Wiche.** 1997. Targeted inactivation of plectin reveals essential function in maintaining the integrity of skin, muscle, and heart cytoarchitecture. Genes Dev. **11:**3143–3156.
2. **Coulombe, P. A.** 1997. Towards a molecular definition of keratinocyte acti-

vation after acute injury to stratified epithelia. Biochem. Biophys. Res. Commun. **236:**231–238.
3. **Coulombe, P. A.** 2003. Wound epithelialization: accelerating the pace of discovery. J. Investig. Dermatol. **37:**219–230.
4. **Fässler, R., and M. Meyer.** 1995. Consequences of lack of beta 1 integrin gene expression in mice. Genes Dev. **9:**1896–1908.
5. **Fujiwara, S., H. Shinkai, S. Takayasu, K. Owaribe, S. Tsukita, and T. Kageshita.** 1992. A case of subepidermal blister disease associated with autoantibody against 450kD protein. J. Dermatol. **19:**610–613.
6. **Fujiwara, S., K. Kohno, A. Iwamatsu, I. Naito, and H. Shinkai.** 1996. Identification of a 450-kDa human epidermal autoantigen as a new member of the plectin family. J. Investig. Dermatol. **106:**1125–1130.
7. **Fujiwara, S., N. Takeo, Y. Otani, D. A. D. Parry, M. Kunimatsu, R. Lu, M. Sasaki, N. Matsuo, M. Khaleduzzaman, and H. Yoshioka.** 2001. Epiplakin, a novel member of the plakin family originally identified as a 450-kDa human epidermal autoantigen. J. Biol. Chem. **276:**13340–13347.
8. **Green, K. J., D. A. D. Parry, P. M. Steinert, M. L. A. Virata, R. M. Wagner, B. D. Angst, and L. A. Nilles.** 1990. Structure of the human desmoplakins. Implications for function in the desmosomal plaque. J. Biol. Chem. **265:** 2603–2612.
9. **Guo, L., L. Degenstein, J. Dowling, Q.-C. Yu, R. Wollmann, B. Perman, and E. Fuchs.** 1995. Gene targeting of BPAG1: abnormalities in mechanical strength and cell migration in stratified epithelia and neurologic degeneration. Cell **81:**233–243.
10. **Jang, S.-I., A. Kalinin, K. Takahashi, L. N. Marekov, and P. M. Steinert.** 2005. Characterization of human epiplakin: RNAi-mediated epiplakin depletion leads to the disruption of keratin and vimentin IF networks. J. Cell Sci. **118:**781–793.
11. **Kodama, A., T. Lechler, and E. Fuchs.** 2004. Coordinating cytoskeletal tracks to polarize cellular movements. J. Cell Biol. **167:**203–207.
12. **Leung, C. L., D. Sun, and R. K. H. Liem.** 1999. The intermediate filament protein peripherin is the specific interaction partner of mouse BPAG1-n (Dystonin) in neurons. J. Cell Biol. **144:**435–446.
13. **Leung, C. L., K. J. Green, and R. K. H. Liem.** 2002. Plakins: a family of versatile cytolinker proteins. Trends Cell Biol. **12:**37–45.
14. **Martin, P.** 1997. Wound healing—aiming for perfect skin regeneration. Science **276:**75–81.
15. **Mazzalupo, S., M. J. Wawersik, and P. A. Coulumbe.** 2002. An ex vivo assay to assess the potential of skin keratinocytes for wound epithelialization. J. Investig. Dermatol. **118:**866–870.
16. **McLean, W. H., L. Pulkkinen, F. J. Smith, E. L. Rugg, E. B. Lane, F. Bullrich, R. E. Burgeson, S. Amano, D. L. Hudson, K. Owaribe, J. A. McGrath, J. R. McMillan, R. A. Eady, I. M. Leigh, A. M. Christiano, and J. Uitto.** 1996. Loss of plectin causes epidermolysis bullosa with muscular dystrophy: cDNA cloning and genomic organization. Genes Dev. **10:**1724–1735.
17. **Meng, J.-J., E. A. Bornslaeger, K. J. Green, P. M. Steinert, and W. Ip.** 1997. Two-hybrid analysis reveals fundamental differences in direct interactions between desmoplakin and cell type-specific intermediate filaments. J. Biol. Chem. **272:**21495–21503.
18. **Nikolic, B., E. M. Nulty, B. Mir, and G. Wiche.** 1996. Basic amino acid residue cluster within nuclear targeting sequence motif is essential for cytoplasmic plectin-vimentin network junctions. J. Cell Biol. **134:**1455–1467.
19. **Paladini, R. D., K. Takahashi, N. S. Bravo, and P. A. Coulombe.** 1996. Onset of re-epithelialization after skin injury correlates with a reorganization of keratin filaments in wound edge keratinocytes: defining a potential role for keratin 16. J. Cell Biol. **132:**381–397.
20. **Röper, K., S. L. Gregory, and N. H. Brown.** 2002. The 'Spectraplakins': cytoskeletal giants with characteristics of both spectrin and plakin families. J. Cell Sci. **115:**4215–4225.
21. **Spazierer, D., P. Fuchs, V. Pröll, L. Janda, S. Oehler, I. Fischer, R. Hauptmann, and G. Wiche.** 2003. Epiplakin gene analysis in mouse reveals a single exon encoding a 725-kDa protein with expression restricted to epithelial tissues. J. Biol. Chem. **278:**31657–31666.
22. **Stappenbeck, T. S., E. A. Bornslaeger, C. M. Corcoran, H. H. Luu, M. L. Virata, and K. J. Green.** 1993. Functional analysis of desmoplakin domains: specification of the interaction with keratin versus vimentin intermediate filament networks. J. Cell Biol. **123:**691–705.
23. **Steinböck, F. A., B. Nikolic, P. A. Coulombe, E. Fuchs, P. Traub, and G. Wiche.** 2000. Dose-dependent linkage, assembly inhibition and disassembly of vimentin and cytokeratin 5/14 filaments through plectin's intermediate filament-binding domain. J. Cell Sci. **113:**483–491.
24. **Steinert, P. M., D. A. D. Parry, and L. N. Marekov.** 2003. Trichohyalin mechanically strengthens the hair follicle. J. Biol. Chem. **278:**41409–41419.
25. **Takeo, N., W. Wang, N. Matsuo, H. Sumiyoshi, H. Yoshioka, and S. Fujiwara.** 2003. Structure and heterogeneity of the human gene for epiplakin (EPPK1). J. Investig. Dermatol. **121:**1224–1226.
26. **Wawersik, M., and P. A. Coulombe.** 2000. Forced expression of keratin 16 alters the adhesion, differentiation, and migration of mouse skin keratinocytes. Mol. Biol. Cell **11:**3315–3327.
27. **Wawersik, M. J., S. Mazzalupo, D. Nguyen, and P. A. Coulombe.** 2001. Increased levels of keratin 16 alter epithelialization potential of mouse skin keratinocytes in vivo and ex vivo. Mol. Biol. Cell **12:**3439–3450.
28. **Wiche, G., D. Gromov, A. Donovan, M. J. Castanon, and E. Fuchs.** 1993. Expression of plectin mutant cDNA in cultured cells indicates a role of COOH-terminal domain in intermediate filament association. J. Cell Biol. **121:**607–619.
29. **Wong, P., E. Colucci-Guyon, K. Takahashi, C. Gu, C. Babinet, and P. A. Coulombe.** 2000. Introducing a null mutation in the mouse K6α and K6β genes reveals their essential structural role in the oral mucosa. J. Cell Biol. **150:**921–928.
30. **Wong, P., and P. A. Coulombe.** 2003. Loss of keratin 6 (K6) proteins reveals a function for intermediate filaments during wound repair. J. Cell Biol. **163:**327–337.
31. **Yamamoto-Hino, M., A. Miyawaki, A. Segawa, E. Adachi, S. Yamashina, T. Fujimoto, T. Sugiyama, T. Furuichi, M. Hasegawa, and K. Mikoshiba.** 1998. Apical vesicles bearing inositol 1,4,5-triphosphate receptors in the Ca^{2+} initiation site of ductal epithelium of submandibular gland. J. Cell Biol. **141:**135–142.